

1 **Body-size and food-web interactions mediate species range shifts under warming**

2
3 E. W. Tekwa^{1,2,3}, James R. Watson⁴, Malin L. Pinsky¹

4 ¹Department of Ecology, Evolution, and Natural Resources, Rutgers University, New
5 Brunswick, NJ, USA

6 ²Department of Ecology and Evolutionary Biology, Princeton University, Princeton, NJ, USA

7 ³Department of Zoology, University of British Columbia, BC, Canada

8 ⁴College of Earth, Ocean and Atmospheric Sciences, Oregon State University, Corvallis, OR,
9 USA

10 11 **Abstract**

12 Species ranges are shifting in response to climate change, but most predictions disregard
13 food-web interactions and, in particular, if and how such interactions change through time.
14 Predator-prey interactions could speed up species range shifts through enemy release or create
15 lags through biotic resistance. Here, we developed a spatially explicit model of interacting
16 species, each with a thermal niche and embedded in a size-structured food-web across a
17 temperature gradient that was then exposed to warming. We also created counterfactual single
18 species models to contrast and highlight the effect of trophic interactions on range shifts. We
19 found that dynamic trophic interactions hampered species range shifts across 450 simulated food
20 webs with up to 200 species each over 200 years of warming. All species experiencing dynamic
21 trophic interactions shifted more slowly than single-species models would predict. In addition,
22 the trailing edges of larger-bodied species ranges shifted especially slowly because of ecological
23 subsidies from small shifting prey. Trophic interactions also reduced the numbers of locally
24 novel species, novel interactions, and productive species, thus maintaining historical community
25 compositions for longer. Current forecasts ignoring dynamic food-web interactions and
26 allometry may overestimate species' tendency to track climate change.

27 28 **Keywords**

29 Range shift, marine food web, climate change, metabolic theory, body size, extinction debt

30 31 **Introduction**

32 Species ranges are shifting in response to climate change and variability [1–3]. These
33 spatial shifts in species ranges are having an impact on ecosystem functions [4,5] and the
34 provision of ecosystem services with subsequent impacts on local economies [6]. Most efforts to
35 project how and why species ranges are shifting have focused on the direct impacts of climate
36 change on individual species [7–9]. These “one at a time” species projections reveal substantial
37 potential for reorganized and novel community compositions [10,11]. However, food-web
38 interactions among species can also affect the rate and direction of species range shifts [12–14].
39 A key lesson so far is that competition can keep species from shifting with warming [12], a
40 prediction recently corroborated experimentally [15]. However, much less is known about how
41 the combination of trophic interactions and warming simultaneously affect geographic shifts in
42 species ranges, despite their anticipated importance [16]. To date, most spatially explicit studies
43 of species range shifts have not accounted for changes in trophic interactions in a warming world
44 [17–19].

45 Several food-webs characteristics are likely to be important for species range shift under
46 warming. Empirical evidence suggests that many food-webs are strongly organized by body size

47 as well as by temperature, particularly those in marine environments [20,21]. Body size and
48 temperature both mediate organismal metabolic rates and trophic interactions [22]. In these
49 communities, mortality imposed by predators [23] and competition for prey may prevent novel
50 species from invading, processes that fall under the term biotic resistance [24–26]. Alternatively,
51 small prey that escape traditional predators—either because predators are specialists or are the
52 first to decline [27]—may accelerate prey leading edge shifts more than larger predators, which
53 has been termed enemy or predator release [28]. Large-scale comparative studies show
54 ambiguous patterns regarding size or trophic differences in species range-shifts, potentially
55 because hypotheses have been vague and challenging to test [29,2]. Developing clear
56 expectations for the influence of food-web interactions on species range shifts will help with the
57 specification of more precise and testable hypotheses.

58 Here, we have developed a dynamic and spatially explicit food-web model that is based
59 on allometric and metabolic relationships. We use this model to develop new theory and insight
60 into how trophic interactions, and their re-organization through time and space, affect species
61 range shifts under warming. Multi-species food webs (not just food chains [30]) of multiple
62 trophic levels can emerge in this model from dispersal and the differences among species in body
63 sizes and thermal preferences (see [10]). To complement this model, we also created a set of
64 single-species counterfactual models to clarify expectations in the absence of dynamic trophic
65 interactions. Our results reveal that trophic interactions slow down the rate of species range
66 shifts, suggesting that most studies of future range shifts overestimate how well species will
67 track changing climates.

68

69 **Methods**

70 To explore the influence of species interactions on species range shifts, we developed a
71 discrete-time and discrete-space food-web model (Eq. 1). This food-web model was initialized
72 with a basal resource with body size 10^{-2} g and $N=200$ heterotroph species distributed across 21
73 spatial patches x . Temperature across patches at time $t=0$ spanned 4 to 24 °C (1 °C per patch) to
74 roughly represent a transect from pole to equator (Figure 1A). Each patch was a square with
75 sides measuring 471 km. Each species was assigned a body size s_i (\log_{10} -uniformly random
76 between 10^0 and 10^6 g) and optimal temperature for searching prey $T_{i,opt}$ (uniformly random
77 between 0 and 34 °C). Heterotrophs from species i in patch x of biomass B_{ix} consumed the basal
78 resource (which is described in more detail below) and other species with efficiency λ and at rate
79 f_{ijx} that depended on relative predator (i) – prey (j) body sizes [31] while also experiencing a
80 body-size- and temperature-dependent metabolic cost D_{ix} [32] and while dispersing to each
81 adjacent patch at a rate κ day $^{-1}$ (or fraction of biomass dispersed per day). The cross-patch
82 dispersal rate κ was related to the diffusion coefficient m (Table 1:T3), which was varied at the
83 same levels across all species for the simulation experiments (Table 2). Empirical observation
84 support no or even negative relationships between body size and dispersal or correlates of
85 dispersal [33,34], including no correlation between offspring size and pelagic larval duration
86 [35]. Even though swim speed increases with size [36], it remains unclear how linear speed
87 translates into dispersal because species have different tendencies to return home. Nevertheless,
88 we also relaxed the assumption of size-independent dispersal in a sensitivity test (see Eq. A2 in
89 Supplementary Appendix A). For the main results, we used κ values of 0, 4.5×10^{-12} , 4.5×10^{-9} ,
90 4.5×10^{-6} , 4.5×10^{-5} , and 4.5×10^{-4} day $^{-1}$. Dispersal rates above these generated unrealistic results.
91 For simplicity, we labelled dispersal rates in figures only by magnitudes (omitting the 4.5
92 multiplier). κ was set to zero at both ends of the patch array.

93

94 Eq. 1

$$\frac{\Delta B_{ix}}{\Delta t} = \frac{B_{ix}(t+1) - B_{ix}(t)}{\Delta t} = \sum_{j=0, j \neq i}^N \left[\underbrace{\lambda B_{ix} f_{ijx}(B_{jx})}_{\text{consumption}} - \underbrace{B_{jx} f_{jix}(B_{ix})}_{\text{predation}} \right] - \underbrace{D_{ix} B_{ix}}_{\text{metabolism}} - \underbrace{2\kappa B_{ix}}_{\text{emigration}} + \underbrace{\sum_{y=x \pm 1} \kappa B_{iy}}_{\text{immigration}} \text{ [gm}^{-3}\text{ day}^{-1}\text{]}$$

95

96

97 The basal resource grew chemostatically without temperature dependence (Table 1:T1)
 98 and an initial biomass equal to the maximum biomass of 5 gm⁻³, which is around the upper
 99 bound of global mesozooplankton estimates (after wet weight conversion) [37]. It may be
 100 reasonable to assume that basal growth and maximum biomass are relatively temperature
 101 independent compared to individual heterotrophs (fish), since organisms of around 10⁻² g in size
 102 have similar biomass across latitude [37]. We do not address complexity at or below the basal
 103 level; instead we aim for a stable representation of this food web component. Heterotroph
 104 species consumed according to a Type III functional response (f_{ijx}) (Table 1:T2) with search rate
 105 v_{ijx} and handling time τ_{ix} [38] (Table 1:T6 and T7). We chose a Type III because of its stabilizing
 106 properties that generate realistic food web complexity and species richness [39]. The search rate
 107 v_{ijx} of predator i on prey j was a skew normal function of temperature T_x (Table 1:T15) such that
 108 consumers could not feed if they were far from their optimal temperature. Production of a
 109 species was defined as consumption minus predation across all patches, which equaled the rate
 110 of biomass loss to predation (see Eq. A3 in Supplementary Appendix A). Table 1 contains the
 111 detailed equations and Table 2 provides definitions, values, and references for parameters
 112 corresponding to a typical ectotherm marine food-web. A detailed explanation of the equations in
 113 Table 1 is provided in the Supplementary Appendix A. In summary, metabolic cost rises with
 114 size and temperature, handling time decreases with predator size and temperature, and search
 115 rate decreases with predator size and is maximized at preferred prey size and temperature (Figure
 116 1A).

117 The model was run forward at daily timesteps for 1600 to 2400 years (varied randomly to
 118 avoid phase effects of any potential cycles) with stationary temperatures. This “spin-up” phase
 119 was used so that population dynamics settled into a quasi-equilibrium, similarly to how Earth
 120 System Models are initialized [40]. The daily timesteps are comparable to other large marine
 121 ecosystem models [41], which not only accounts for the short generation time of smaller
 122 organisms, but also describes feeding and metabolism dynamics. After this spin-up period, which
 123 was observed to maintain stable biomass trajectories across a reasonably high species diversity
 124 of three trophic levels, gradual warming was imposed as a 3 °C warming over 200 years at all
 125 patches (Figure 1B&C). The warming scenario was in line with current ocean warming
 126 projections [42]. We replicated these simulations 40 times with independent log-uniformly
 127 random initial biomass for each species and patch between 2.2x10⁻¹⁵ and 2.2x10⁻¹⁰ gm⁻³.

128 During the simulations, we recorded shifts in the centroid of each species’ range (a
 129 species’ average location weighted by biomass), leading range edge (2.5th quantile of biomass
 130 starting from the coldest patch), trailing range edge (97.5th quantile biomass), and range size
 131 (patches from leading to trailing edge). Given the spatial gradient in temperatures, isotherms
 132 shifted three patches towards the cold region, so a 100% range shift corresponded to a three-
 133 patch shift. We also recorded the percentage of the local species and species pairs that were
 134 novel or that were extirpated after warming, with presence meaning a local biomass above the
 135 floating-point error (2.2x10⁻¹⁶ gm⁻³ in Matlab). The percentage of novel species pairs was 100

136 times the global number of species pairs that were found together in any patch after but not
 137 before warming, divided by the sum of coexisting pairs after warming. The percentage of
 138 extirpated species pairs was 100 times the global number of species pairs that were found
 139 together in any patch before warming but lost after warming, divided by the sum of coexisting
 140 pairs before warming. For size-specific analyses, we divided the results into small species (10^2 to
 141 10^3 g body-weight) and large species (10^5 to 10^6 g body-weight). Species with leading edges in
 142 the coldest three patches before warming were omitted from the analyses to avoid edge effects,
 143 since these species would run out of room to track a 3 °C warming.

144 For comparison, we fit counterfactual single-species models to species biomass outcomes
 145 during the no-warming spin-up period in the food-web models, except that dynamic trophic
 146 interactions were removed (Eq. 2). These models capture the single-species equivalent of
 147 dynamics in food webs, which can then be used to project what is expected if only species
 148 characteristics and not food web interactions respond dynamically to warming. Each species
 149 experienced metabolic costs and relative intrinsic growth just as specified in the food-web
 150 models. However, temporally constant maximum (intrinsic) growth rates (r_i) and self-
 151 competition (a_i) rates were specified instead of dynamic consumption and predation terms,
 152 consistent with a single species model:

153
 154 Eq. 2
$$\frac{\Delta \tilde{B}_{ix}}{\Delta t} = \tilde{B}_{ix}(r_i \omega_{ix} - D_{ix} - a_i \tilde{B}_{ix}) \quad [\text{gm}^{-3} \text{day}^{-1}]$$

155
 156 Biomass was labelled with tilde to distinguish the counterfactual projections from the
 157 food web outcomes. We included a skew normal function ω_{ix} of temperature T_x (Table 1:T15) so
 158 that realized growth rate declined to zero if species were far from their optimal temperature. To
 159 estimate the two parameters r_i and a_i that best matched the species in the food-web models, we
 160 needed to match long-run production in addition to biomass (two equations to solve for two
 161 parameters). We defined production \tilde{P}_{ix} in the model as growth minus metabolic cost and a
 162 portion ($1/c$) of intraspecific competition. We partitioned intraspecific competition this way
 163 because, by definition, competition can come from either suppressed birth and growth or
 164 increased mortality, the latter being interpreted here as production through a loss effect attributed
 165 to conspecifics.

166
 167 Eq. 3
$$\tilde{P}_{ix} = \tilde{B}_{ix} \left(r_i \omega_{ix} - D_{ix} - \frac{a_i}{c} \tilde{B}_{ix} \right) \quad [\text{gm}^{-3} \text{day}^{-1}]$$

168
 169 In this formulation, c controls whether competition results in production due to increased
 170 mortality ($c=\infty$), no production due to suppressed birth ($c=1$, which also implies no net
 171 production in Eq. 3), or somewhere in between. For each species i from the food-web
 172 simulations, we recorded the average biomass and average production (consumption minus
 173 metabolism) from the transient no-warming period of the food-web simulation. We then fit the
 174 model's equilibrium biomass (from solving Eq. 2) and production (Eq. 3) against these modeled
 175 data after fixing c for all species. We repeated this across a range of c to find the value that
 176 produced the closest match between the aggregate community biomass and production and the
 177 food-web's total biomass and production (minimum sum of squares divided by each variable's
 178 magnitude) (Table S1). This phenomenological single-species model resembles what a scientist
 179 might do with historical data if trying to project single species shifts during the warming period.
 180 This model can also be understood as a counterfactual to the food-web model, one with similar
 181 species biomasses and productions but with dynamic trophic interactions taken out (Figure S2).

182 The sensitivity of the single-species projections to parameterization was tested using two
183 alternative values of c that underestimated and overestimated production (Table S1), which
184 should respectively underestimate and overestimate intrinsic growth rate, a key parameter that
185 could influence shifting rates.

186 We explored the sensitivity of our food-web results by also using alternative values for
187 the reference predator-prey mass ratio α_R , the activation energy E_a , the fraction of time hunting
188 F_h , the consumption efficiency λ (see Table 2), and the size dependence of dispersal rate κ .
189 These alternative values included, respectively, the lower end of α_R [31], the E_a corresponding to
190 all organisms rather than ectotherms only [32], half of the original F_h [43], half of the original λ
191 [44], and a κ that increased with size based on swim speed [36] (Supplementary Appendix A).
192 We also explored randomly defining $P_N=10$ to 50% of all prey as inedible independently for each
193 predator, which increased specialization and the potential for enemy release of prey (Table 2).
194 Higher specialization led to food web collapse. Finally, we conducted fine-resolution sensitivity
195 analyses on α_R , E_a , and κ (Table 2). For each alternative parameter value, 10 replicates were run
196 at the mean dispersal rate of 10^{-12} day⁻¹. In sum, 21x10 food webs were simulated for sensitivity
197 tests, bring the total simulations including those in the main analysis to 450 food webs.

198

199 Results

200 Under warming, the food-web model revealed aggregate biomass shifting toward the
201 colder regions, as expected (Figure 1B & D). Snapshots of food web structure (mapped by the
202 two traits of body size and optimal search temperature) over space and time revealed that some
203 part of the original local communities (blue in Figure 1H) shifted together (shown as red in
204 Figure 1E), while other species shifted less or even stayed in their original patches to rewire
205 incoming communities (overlapping blue and red species in Figure 1E). There is also evidence of
206 enemy release, as one species moved from low biomass in its original patch (sp.1 in Figure 1H)
207 to high biomass (Figure 1F&G). Even though larger predators of sp. 1 were present in its new
208 thermally optimal patch (Figure 1E), they were saturated by the availability of other prey that
209 were at a more optimal size for foraging.

210 Range sizes before warming averaged from 1.4 to 5.2 patches as dispersal rate increased
211 from 0 to 10^{-4} (with larger increase for larger species, Figure S1), corresponding to distances of
212 1000 to 4000 km that are typical for marine species [45]. On average, species' centroids, leading
213 edges, and trailing edges tracked thermal shifts more closely at higher dispersal rates (Figure 2A,
214 C, D, solid blue curves). Species range sizes, on the other hand, on average contracted for slow
215 dispersal rates and expanded for rapid dispersal rates (Fig. 2B, solid blue curve).

216 Across body sizes, all species exhibited similar leading edge shifts (Figure 2C solid
217 curves), but centroids and trailing edges shifted much more for small (10^2 to 10^3 g body-weight)
218 than large (10^5 to 10^6 g body-weight) sized species (Figure 2A, D solid cyan vs. red curves).
219 These differences in trailing edge dynamics for large and small species meant that ranges among
220 small species contracted at slow dispersal rates, while large species ranges expanded at all but
221 zero dispersal rates.

222 In the food-web model, locally novel species and novel species pairs (pairs that coexist in
223 any patch) were more common at intermediate dispersal rates (Figure 2E, F solid blue curves). In
224 contrast, the highest percentage of species experienced local extirpation and the highest
225 percentage of historical species-pairs were lost at low dispersal rates (Figure 2G, H solid blue
226 curves). Large species were more likely to begin coexisting with novel species than were small
227 species (Figure 2F solid cyan vs. red curves), consistent with the lag in trailing edge range shifts

228 among large species. Small species were more likely to be locally extirpated than were large
229 species, also consistent with lags in large species' trailing edges (Figure 2G solid cyan vs. red
230 curves). Similarly, historical pairs of coexisting small species were more likely to be lost than
231 pairs of large species at low dispersal rates (Figure 2H solid cyan vs. red curves).

232 The single-species counterfactual models suggested that, in the absence of dynamic
233 predator-prey interactions, all species would closely match the thermal shift even at the lowest
234 non-zero dispersal rate (Figure 2A, C, D dashed curves). In addition, single-species models only
235 predicted substantial range contractions for a zero dispersal rate (Figure 2B dashed curves).
236 Compared to the food-web model, single-species models over-predicted the distance that species
237 shifted (Figure 2E, G, H) and under-predicted changes in range size (Figure 2F). Single species
238 models also over-predicted the percentage of locally novel species and of novel species pairs as
239 compared to the full food-web dynamics (Figure 2E, G). Finally, single-species models failed to
240 resolve the large differences among body sizes in distance shifted, unlike for the food-web
241 models in which larger species tended to shift their trailing edge less and expand range size more
242 (Figure 2). The lack of body-size differences in range shifts appeared even though the single-
243 species model assumed that intrinsic growth rate r_i was a decreasing function of size across all
244 simulations (Eq. 2), consistent with metabolic theory that was also embedded in the food-web
245 model.

246 Community aggregate statistics showed differences in overall stock, flow, and diversity
247 metrics between food-web and single-species projections under warming. Community biomass
248 and production increased in the food-web model after warming at dispersal rates higher than 10^{-12}
249 day^{-1} (Figure S3A & B). In contrast, the single species model projected on average little to no
250 changes to biomass and production after warming, along with large differences in production
251 changes across replicates. However, these food-web changes were accompanied by a greater
252 number of species that became unproductive (production < 0) after warming, whereas the single-
253 species model showed no increase in unproductive species at all non-zero dispersal rates (Figure
254 S3C). Since production is consumption minus metabolic cost, and all other terms (not counting
255 migration since production here is computed globally) contributed negatively to net growth in
256 Eq. 1, any existing unproductive species were on extinction trajectories – although they may
257 have had non-extinction equilibria, especially if temperatures stabilized again during the
258 protracted transient periods [46]. In any case, the modeled food-webs had a longer transient
259 approach to equilibrium than single species projections. Community composition was also
260 impacted by food webs, which showed a decline in mean body size not predicted by single-
261 species projections (Figure S3D). In term of biodiversity metrics, both food-web and single-
262 species projections agreed only a few global extinctions would occur at non-zero dispersal rates
263 (Figure S3E). Average alpha diversity, or local richness, showed an increase at intermediate
264 dispersal rates and a decrease otherwise (Figure S3F).

265 Metrics of trophic level in conjunction with diversity suggest that the model generated
266 qualitatively realistic food webs. At all non-zero dispersal rates, local richness was much higher
267 than mean and maximum trophic levels of 2.6 and 3 with 1 being the basal level, which remained
268 similar before and after warming (Figure S3G&H). This result meant that multiple species shared
269 similar trophic levels and formed food webs rather than food chains. With no dispersal, simple
270 food webs of about 5 species spanning two heterotrophic levels still emerged initially, but after
271 warming they approached food chains (two species). These results gave confidence that our
272 model effectively captured known features of natural food webs.

273 The single-species shift projections were insensitive to alternative values of the parameter
274 c that controlled production (see Table S1; results indistinguishable from Figure 1). Sensitivity
275 analyses that changed the portion of potential prey being inedible P_N for each species (i.e., more
276 specialists when $P_N > 0$), the activation energy E_a , the reference predator-prey mass ratio α_R , the
277 fraction of time hunting F_h , the consumption efficiency λ (Table 2), and size-dependent dispersal
278 rate κ (Supplementary Appendix A) affected the magnitude of shifts and assemblage changes,
279 but they had little to no impact on the ordering of the changes by body size or food-web vs.
280 single-species models (Figure S4-S8). The notable exceptions were in leading edge shifts, for
281 which low activation energy, low or high predator-prey mass ratios, and high levels of inedible
282 prey reversed the trends from being slightly lower to slightly higher for smaller species relative
283 to larger species (Figures S5C, S6C, S7C). In term of magnitude of shifts, the results were most
284 sensitive to activation energy, with values lower than expected for marine ecosystems creating
285 species shifts that were quite similar to single-species projections (Figure S4F). The sensitivity
286 tests suggested that food-web interactions generally impede species range shifts under warming,
287 and more so for large predatory species, across plausible assumptions about food-web structure
288 and dispersal rates.

289 Discussion

291 We developed a spatially explicit food-web model and a set of single-species
292 counterfactual models to explore the role of species interactions in either facilitating or hindering
293 species range shifts in a warming world. The results of the food-web model revealed that
294 dynamic trophic interactions overall hamper species' abilities to shift their spatial distributions in
295 response to warming temperatures at both leading and trailing range edges. In addition, trophic
296 interactions created differences among species of different trophic levels, with larger-bodied top
297 predators persisting longer than smaller prey in historical habitats. These delayed extirpations
298 created a lag in the trailing edge shift and an overall range expansion for these large species. In
299 contrast, smaller bodied species experienced a contraction in their spatial distributions. Diversity,
300 range size, trophic level outcomes, and snapshots of species relationships all resembled
301 qualitative features of real food webs. These results highlight the importance of accounting for
302 both spatial dispersal and trophic interactions when considering the impact of climate change on
303 species ranges and assemblages.

304 Dynamic trophic interactions slowed species' range shifts compared to expectations from
305 single-species models. This result complements previous theoretical studies showing that
306 competition can limit range shifts [23,12] and suggests that biotic resistance processes [25,26]
307 are likely to be stronger than enemy release effects on range shifts [28]. We found this pattern
308 even when a high portion of potential prey were inedible, a scenario that allowed for more
309 opportunities to escape enemies. High levels of inedible prey did lead to greater leading edge
310 shifts among smaller as compared to larger species, as expected from enemy release, but this did
311 not alter the overall shift lags imposed by food webs. Our results also complement models
312 suggesting that competition among predators for prey will slow down range shifts [47]. In nature,
313 it is difficult to isolate food-web effects, but one approach is to compare communities in
314 protected area with those not in such areas, with protection generally preserving stronger
315 predation processes. In temperate reef communities protected from fishing, for example, high-
316 trophic-level species are more abundant than in unprotected communities [25]. Despite warming
317 water, these protected communities had fewer biodiversity changes and fewer colonizations by

318 novel species, as compared to unprotected communities [25]. The example appears to support the
319 theoretical prediction that natural food-web interactions would slow range shifts.

320 Smaller species shifted more than larger species in terms of centroids and trailing edges,
321 resulting in range contraction across a wide range of dispersal rates that contrasted with range
322 expansion for larger species. This difference could occur because smaller species have higher
323 metabolic rates, faster generation times, and therefore faster extirpation from patches that are no
324 longer suitable due to warming. However, our counterfactual single-species model that also
325 incorporated higher metabolic rate in smaller species did not show a large difference in shift
326 patterns across size, suggesting that a size-metabolism explanation is not sufficient.

327 Instead, food-web interactions are a stronger explanation for the lag among larger bodied
328 species. Smaller species preyed to a greater extent upon a basal resource that was not
329 temperature sensitive. Consequently, the primary limit on small heterotrophs' growth was their
330 own temperature-sensitive search rate. In nature, small marine organisms that heterotrophs
331 depend on may indeed be relatively temperature insensitive due to high species diversity [48]
332 and genetic diversity [49] that assist in adaptation to changing conditions. However, nutrient and
333 ecosystem dynamics also modulate small organisms in nature, which we did not examine in our
334 model [50]. In contrast, larger species near their trailing range edge were subsidized by novel
335 prey that expanded into new habitat (despite also facing the same temperature-dependent feeding
336 limitations that smaller species experienced). The increase that we observed in community
337 biomass and production in food-webs after warming likely reflects the same process. Since large
338 species had no production (they were not consumed), the increase in community production can
339 be attributed to smaller species. This influx of smaller species as prey at the trailing edges of
340 large species would have helped prevent predator extirpation. This phenomenon may be further
341 amplified if prey defense evolution is also considered, since prey are likely to be naïve to novel
342 predators [51].

343 The ecological subsidy from colonizing species that benefits top predators would not
344 appear in closed food-webs without the possibility of colonization. Closed food webs generally
345 suggest that top predators are the most vulnerable to changing climate [27]. The persistence of
346 large predators in their historically occupied patches, in turn, imposed a top-down control that
347 slowed the rate of colonization by small prey relative to models without food-web interactions.
348 This effect is consistent with previous findings that predators have larger effects near species
349 range edges [52]. These predicted differences among species also align with empirical studies
350 that find faster shifts in species centroids among small species [2,53].

351 Although warming led to novel local assemblages (coexisting species-pairs) in both the
352 trophic and single-species models, the presence of dynamic trophic interactions led to fewer
353 ecologically novel species assemblages. This finding is contrary to effects from competitive
354 interactions, which predicted more novel assemblages [12]. Changes in local and global richness
355 were generally small and similar between food web and single-species projections. The
356 extinction pattern differs from previous theoretical works, which found extinction to be
357 exacerbated by competitive species interactions [54]. These results highlight important
358 differences in the ecological consequences of competitive versus trophic interactions for range
359 shifts and future communities.

360 Even though lags in range shifts persisted over 200 years of warming in our simulations,
361 the increase in non-productive species among warming food-webs suggested that some species,
362 particularly large species, may eventually have experienced more rapid extirpation at their
363 trailing edges. Compared to the single-species model, the food-web model suggested longer

364 transient dynamics [46] and extinction debt [55], making non-equilibrium phenomena more
365 important than in hypothetical non-trophic communities.

366 We modelled food webs across a size range that corresponds to heterotrophic, size-
367 structured food webs characteristic of marine fish communities, which have been a common
368 focus in ecological modelling [56]. However, size and temperature dependent metabolic theory
369 can be extended to smaller sizes, including the basal planktonic class [57]. Future research
370 incorporating a larger size range in food web models would introduce both computational and
371 theoretical challenges because of different generation times and error propagation from low to
372 high trophic levels. However, proper inclusion of smaller organisms would also clarify the role
373 of bottom-up contributions to geographic shifts [58]. While we saw that size dependence of
374 dispersal across species did not appreciably affect range shift patterns, differences across life
375 stages may mediate trophic interactions, which can be addressed through individual based or
376 age-structured modelling. Moving forward, range shift projections will be more informative
377 when human action [59] and genetic evolution [54] are coupled with ecological dynamics.

378 Our results show that projecting species range shifts based on single-species distribution
379 models [9] will likely overestimate any given species' tendency to keep track with climate
380 change. Thus, dynamic trophic interactions and body size are important factors for ecological
381 projections under changing environments.
382

383 **Acknowledgments**

384 We thank Charles A. Stock, Anieke van Leeuwen, Ken H. Andersen, Emily Moberg, Rebecca L.
385 Selden, and Matthieu Barbier for discussions. The authors acknowledge the Office of Advanced
386 Research Computing (OARC) at Rutgers for providing access to the Amarel computing cluster.
387

388 **Funding**

389 This work was funded by the Gordon and Betty Moore Foundation (GBMF5502), a Hakai
390 Postdoctoral Fellowship, and NSF awards OCE-1426891, DEB-1616821, and OISE-1743711.
391

392 **Data, code and materials**

393 All Matlab codes are available on GitHub/Zenodo at doi.org/10.5281/zenodo.6374072 [60].
394

395 **Competing interests**

396 The authors declare no competing interests.
397

398 **Authors' contributions**

399 Conceptualization – JW and MP; Formal analysis - ET; Methodology – ET, JW, and MP;
400 Writing – original draft - ET; Writing – review & editing by ET, JW, and MP.

401 **References**

- 402 1. Parmesan C. 2006 Ecological and Evolutionary Responses to Recent Climate Change. *Annu.*
403 *Rev. Ecol. Evol. Syst.* **37**, 637–669. (doi:10.1146/annurev.ecolsys.37.091305.110100)
- 404 2. Pinsky ML, Worm B, Fogarty MJ, Sarmiento JL, Levin SA. 2013 Marine Taxa Track Local
405 Climate Velocities. *Science* **341**, 1239–1242. (doi:10.1126/science.1239352)
- 406 3. Poloczanska ES *et al.* 2013 Global imprint of climate change on marine life. *Nature Clim*
407 *Change* **3**, 919–925. (doi:10.1038/nclimate1958)
- 408 4. Doney SC *et al.* 2012 Climate Change Impacts on Marine Ecosystems. *Annual Review of*
409 *Marine Science* **4**, 11–37. (doi:10.1146/annurev-marine-041911-111611)
- 410 5. Moore JK *et al.* 2018 Sustained climate warming drives declining marine biological
411 productivity. *Science* **359**, 1139–1143. (doi:10.1126/science.aao6379)
- 412 6. Fenichel EP, Levin SA, McCay B, St. Martin K, Abbott JK, Pinsky ML. 2016 Wealth
413 reallocation and sustainability under climate change. *Nature Climate Change* **6**, 237–244.
414 (doi:10.1038/nclimate2871)
- 415 7. Guisan A, Thuiller W. 2005 Predicting species distribution: offering more than simple habitat
416 models. *Ecol Letters* **8**, 993–1009. (doi:10.1111/j.1461-0248.2005.00792.x)
- 417 8. Buckley LB, Urban MC, Angilletta MJ, Crozier LG, Rissler LJ, Sears MW. 2010 Can
418 mechanism inform species' distribution models?: Correlative and mechanistic range models.
419 *Ecology Letters* , no-no. (doi:10.1111/j.1461-0248.2010.01479.x)
- 420 9. Morley JW, Selden RL, Latour RJ, Frölicher TL, Seagraves RJ, Pinsky ML. 2018 Projecting
421 shifts in thermal habitat for 686 species on the North American continental shelf. *PLoS ONE*
422 **13**, e0196127. (doi:10.1371/journal.pone.0196127)
- 423 10. Zhang L, Takahashi D, Hartvig M, Andersen KH. 2017 Food-web dynamics under climate
424 change. *Proceedings of the Royal Society B: Biological Sciences* **284**, 20171772.
425 (doi:10.1098/rspb.2017.1772)
- 426 11. Selden RL, Batt RD, Saba VS, Pinsky ML. 2018 Diversity in thermal affinity among key
427 piscivores buffers impacts of ocean warming on predator-prey interactions. *Glob Change*
428 *Biol* **24**, 117–131. (doi:10.1111/gcb.13838)
- 429 12. Urban MC, Tewksbury JJ, Sheldon KS. 2012 On a collision course: competition and
430 dispersal differences create no-analogue communities and cause extinctions during climate
431 change. *Proceedings of the Royal Society B: Biological Sciences* **279**, 2072–2080.
432 (doi:10.1098/rspb.2011.2367)
- 433 13. Alexander JM, Diez JM, Levine JM. 2015 Novel competitors shape species' responses to
434 climate change. *Nature* **525**, 515–518. (doi:10.1038/nature14952)

- 435 14. Thompson PL, Gonzalez A. 2017 Dispersal governs the reorganization of ecological
436 networks under environmental change. *Nature Ecology & Evolution* **1**, 0162.
437 (doi:10.1038/s41559-017-0162)
- 438 15. Legault G, Bitters ME, Hastings A, Melbourne BA. 2020 Interspecific competition slows
439 range expansion and shapes range boundaries. *Proc Natl Acad Sci USA* **117**, 26854–26860.
440 (doi:10.1073/pnas.2009701117)
- 441 16. Gilman SE, Urban MC, Tewksbury J, Gilchrist GW, Holt RD. 2010 A framework for
442 community interactions under climate change. *Trends in Ecology & Evolution* **25**, 325–331.
443 (doi:10.1016/j.tree.2010.03.002)
- 444 17. Brose U, Dunne JA, Montoya JM, Petchey OL, Schneider FD, Jacob U. 2012 Climate
445 change in size-structured ecosystems. *Phil. Trans. R. Soc. B* **367**, 2903–2912.
446 (doi:10.1098/rstb.2012.0232)
- 447 18. Fussmann KE, Schwarzmüller F, Brose U, Jousset A, Rall BC. 2014 Ecological stability in
448 response to warming. *Nature Clim Change* **4**, 206–210. (doi:10.1038/nclimate2134)
- 449 19. Schwarz B *et al.* 2017 Warming alters energetic structure and function but not resilience of
450 soil food webs. *Nature Clim Change* **7**, 895–900. (doi:10.1038/s41558-017-0002-z)
- 451 20. Riede JO, Binzer A, Brose U, de Castro F, Curtsdotter A, Rall BC, Eklöf A. 2011 Size-based
452 food web characteristics govern the response to species extinctions. *Basic and Applied*
453 *Ecology* **12**, 581–589. (doi:10.1016/j.baae.2011.09.006)
- 454 21. Brose U *et al.* 2019 Predator traits determine food-web architecture across ecosystems. *Nat*
455 *Ecol Evol* **3**, 919–927. (doi:10.1038/s41559-019-0899-x)
- 456 22. Gilbert B *et al.* 2014 A bioenergetic framework for the temperature dependence of trophic
457 interactions. *Ecol Lett* **17**, 902–914. (doi:10.1111/ele.12307)
- 458 23. Holt RD, Barfield M. 2009 Trophic interactions and range limits: the diverse roles of
459 predation. *Proc. R. Soc. B.* **276**, 1435–1442. (doi:10.1098/rspb.2008.1536)
- 460 24. Levine JM, Adler PB, Yelenik SG. 2004 A meta-analysis of biotic resistance to exotic plant
461 invasions: Biotic resistance to plant invasion. *Ecology Letters* **7**, 975–989.
462 (doi:10.1111/j.1461-0248.2004.00657.x)
- 463 25. Bates AE, Barrett NS, Stuart-Smith RD, Holbrook NJ, Thompson PA, Edgar GJ. 2014
464 Resilience and signatures of tropicalization in protected reef fish communities. *Nature Clim*
465 *Change* **4**, 62–67. (doi:10.1038/nclimate2062)
- 466 26. Bates AE, Stuart-Smith RD, Barrett NS, Edgar GJ. 2017 Biological interactions both
467 facilitate and resist climate-related functional change in temperate reef communities. *Proc.*
468 *R. Soc. B.* **284**, 20170484. (doi:10.1098/rspb.2017.0484)

- 469 27. Petchey OL, McPhearson PT, Casey TM, Morin PJ. 1999 Environmental warming alters
470 food-web structure and ecosystem function. *Nature* **402**, 69–72. (doi:10.1038/47023)
- 471 28. Sorte CJB, Williams SL, Carlton JT. 2010 Marine range shifts and species introductions:
472 comparative spread rates and community impacts: Range shifts and non-native species
473 introductions. *Global Ecology and Biogeography* **19**, 303–316. (doi:10.1111/j.1466-
474 8238.2009.00519.x)
- 475 29. Angert AL, Crozier LG, Rissler LJ, Gilman SE, Tewksbury JJ, Chunco AJ. 2011 Do species'
476 traits predict recent shifts at expanding range edges?: Traits and range shifts. *Ecology Letters*
477 **14**, 677–689. (doi:10.1111/j.1461-0248.2011.01620.x)
- 478 30. Barbier M, Loreau M. 2019 Pyramids and cascades: a synthesis of food chain functioning
479 and stability. *Ecology Letters* **22**, 405–419. (doi:10.1111/ele.13196)
- 480 31. Barnes C, Maxwell D, Reuman DC, Jennings S. 2010 Global patterns in predator–prey size
481 relationships reveal size dependency of trophic transfer efficiency. *Ecology* **91**, 222–232.
482 (doi:10.1890/08-2061.1)
- 483 32. Brown JH, Gillooly JF, Allen AP, Savage VM, West GB. 2004 Toward a metabolic theory
484 of ecology. *Ecology* **85**, 1771–1789. (doi:10.1890/03-9000)
- 485 33. Stevens VM *et al.* 2014 A comparative analysis of dispersal syndromes in terrestrial and
486 semi-terrestrial animals. *Ecol Lett* **17**, 1039–1052. (doi:10.1111/ele.12303)
- 487 34. Fenchel T, Finlay BJ. 2004 The Ubiquity of Small Species: Patterns of Local and Global
488 Diversity. *BioScience* **54**, 777. (doi:10.1641/0006-3568(2004)054[0777:TUOSSP]2.0.CO;2)
- 489 35. Bradbury IR, Laurel B, Snelgrove PVR, Bentzen P, Campana SE. 2008 Global patterns in
490 marine dispersal estimates: the influence of geography, taxonomic category and life history.
491 *Proceedings of the Royal Society B: Biological Sciences* **275**, 1803–1809.
492 (doi:10.1098/rspb.2008.0216)
- 493 36. Megrey BA, Rose KA, Klumb RA, Hay DE, Werner FE, Eslinger DL, Smith SL. 2007 A
494 bioenergetics-based population dynamics model of Pacific herring (*Clupea harengus pallasii*)
495 coupled to a lower trophic level nutrient–phytoplankton–zooplankton model: Description,
496 calibration, and sensitivity analysis. *Ecological Modelling* **202**, 144–164.
497 (doi:10.1016/j.ecolmodel.2006.08.020)
- 498 37. Moriarty R, O'Brien TD. 2013 Distribution of mesozooplankton biomass in the global ocean.
499 *Earth System Science Data* **5**, 45–55. (doi:10.5194/essd-5-45-2013)
- 500 38. Holling CS. 1959 Some Characteristics of Simple Types of Predation and Parasitism. *The*
501 *Canadian Entomologist* **91**, 385–398. (doi:10.4039/Ent91385-7)
- 502 39. Rall BC, Guill C, Brose U. 2008 Food-web connectance and predator interference dampen
503 the paradox of enrichment. *Oikos* **117**, 202–213. (doi:10.1111/j.2007.0030-1299.15491.x)

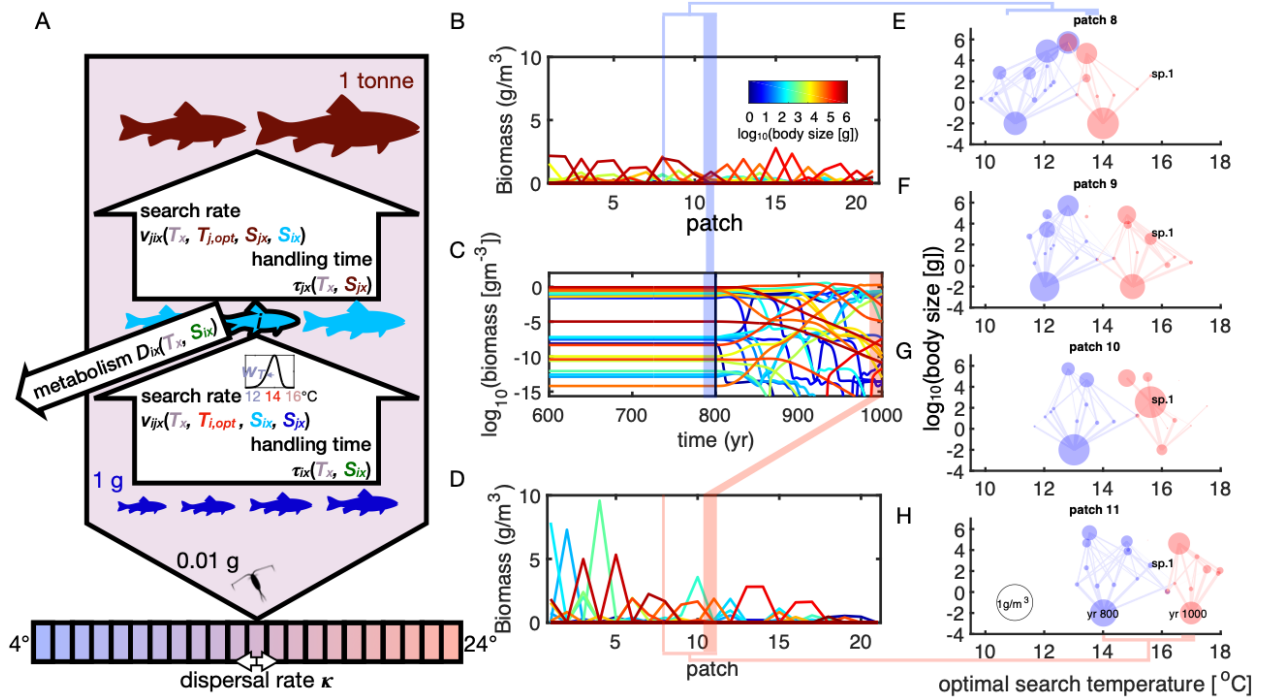
- 504 40. Yool A *et al.* 2020 Spin-up of UK Earth System Model 1 (UKESM1) for CMIP6. *J. Adv.*
505 *Model. Earth Syst.* **12**. (doi:10.1029/2019MS001933)
- 506 41. Pethybridge HR *et al.* 2019 Calibrating process-based marine ecosystem models: An
507 example case using Atlantis. *Ecological Modelling* **412**, 108822.
508 (doi:10.1016/j.ecolmodel.2019.108822)
- 509 42. Cheng L, Abraham J, Hausfather Z, Trenberth KE. 2019 How fast are the oceans warming?
510 *Science* **363**, 128–129. (doi:10.1126/science.aav7619)
- 511 43. Brownscombe J, Gutowsky L, Danylchuk A, Cooke S. 2014 Foraging behaviour and activity
512 of a marine benthivorous fish estimated using tri-axial accelerometer biologgers. *Mar. Ecol.*
513 *Prog. Ser.* **505**, 241–251. (doi:10.3354/meps10786)
- 514 44. Andersen KH, Beyer JE, Lundberg P. 2009 Trophic and individual efficiencies of size-
515 structured communities. *Proceedings of the Royal Society B: Biological Sciences* **276**, 109–
516 114. (doi:10.1098/rspb.2008.0951)
- 517 45. Lester SE, Ruttenberg BI, Gaines SD, Kinlan BP. 2007 The relationship between dispersal
518 ability and geographic range size. *Ecology Letters* **10**, 745–758. (doi:10.1111/j.1461-
519 0248.2007.01070.x)
- 520 46. Hastings A *et al.* 2018 Transient phenomena in ecology. *Science* **361**, eaat6412.
521 (doi:10.1126/science.aat6412)
- 522 47. Fernandes JA, Cheung WWL, Jennings S, Butenschön M, de Mora L, Frölicher TL, Barange
523 M, Grant A. 2013 Modelling the effects of climate change on the distribution and production
524 of marine fishes: accounting for trophic interactions in a dynamic bioclimate envelope
525 model. *Glob Change Biol* **19**, 2596–2607. (doi:10.1111/gcb.12231)
- 526 48. Reuman DC, Gislason H, Barnes C, Mélin F, Jennings S. 2014 The marine diversity
527 spectrum. *Journal of Animal Ecology* **83**, 963–979. (doi:10.1111/1365-2656.12194)
- 528 49. Thomas MK, Kremer CT, Klausmeier CA, Litchman E. 2012 A Global Pattern of Thermal
529 Adaptation in Marine Phytoplankton. *Science* **338**, 1085–1088.
530 (doi:10.1126/science.1224836)
- 531 50. Sarmiento JL *et al.* 2004 Response of ocean ecosystems to climate warming. *Global*
532 *Biogeochem. Cycles* **18**, n/a-n/a. (doi:10.1029/2003GB002134)
- 533 51. Urban MC, Scarpa A, Travis JMJ, Bocedi G. 2019 Maladapted Prey Subsidize Predators and
534 Facilitate Range Expansion. *The American Naturalist* **194**, 590–612. (doi:10.1086/704780)
- 535 52. Boudreau SA, Anderson SC, Worm B. 2015 Top-down and bottom-up forces interact at
536 thermal range extremes on American lobster. *J Anim Ecol* **84**, 840–850. (doi:10.1111/1365-
537 2656.12322)

- 538 53. Perry AL, Low PJ, Ellis JR, Reynolds JD. 2005 Climate Change and Distribution Shifts in
539 Marine Fishes. *Science* **308**, 1912–1915. (doi:10.1126/science.1111322)
- 540 54. Norberg J, Urban MC, Vellend M, Klausmeier CA, Loeuille N. 2012 Eco-evolutionary
541 responses of biodiversity to climate change. *Nature Climate Change* **2**, 747–751.
542 (doi:10.1038/nclimate1588)
- 543 55. Tilman D, May RM, Lehman CL, Nowak MA. 1994 Habitat destruction and the extinction
544 debt. *Nature* **371**, 65–66. (doi:10.1038/371065a0)
- 545 56. Watson JR, Stock CA, Sarmiento JL. 2015 Exploring the role of movement in determining
546 the global distribution of marine biomass using a coupled hydrodynamic – Size-based
547 ecosystem model. *Progress in Oceanography* **138**, 521–532.
548 (doi:10.1016/j.pocean.2014.09.001)
- 549 57. Andersen KH *et al.* 2016 Characteristic Sizes of Life in the Oceans, from Bacteria to
550 Whales. *Annual Review of Marine Science* **8**, 217–241. (doi:10.1146/annurev-marine-
551 122414-034144)
- 552 58. Stock CA *et al.* 2017 Reconciling fisheries catch and ocean productivity. *Proceedings of the*
553 *National Academy of Sciences* **114**, E1441–E1449. (doi:10.1073/pnas.1610238114)
- 554 59. Pinsky ML, Fogarty M. 2012 Lagged social-ecological responses to climate and range shifts
555 in fisheries. *Climatic Change* **115**, 883–891. (doi:10.1007/s10584-012-0599-x)
- 556 60. Tekwa E. 2022 *Code for: Body-size and food-web interactions mediate species range shifts*
557 *under warming*. Zenodo. (doi:10.5281/ZENODO.6374072)
- 558 61. Loreau M, Holt RD. 2004 Spatial Flows and the Regulation of Ecosystems. *The American*
559 *Naturalist* **163**, 606–615. (doi:10.1086/382600)
- 560 62. Ernest SKM *et al.* 2003 Thermodynamic and metabolic effects on the scaling of production
561 and population energy use: Thermodynamic and metabolic effects. *Ecology Letters* **6**, 990–
562 995. (doi:10.1046/j.1461-0248.2003.00526.x)
- 563 63. Colloca F, Carpentieri P, Balestri E, Ardizzone G. 2010 Food resource partitioning in a
564 Mediterranean demersal fish assemblage: the effect of body size and niche width. *Marine*
565 *Biology* **157**, 565–574. (doi:10.1007/s00227-009-1342-7)
- 566 64. Froese R. 2006 Cube law, condition factor and weight-length relationships: history, meta-
567 analysis and recommendations. *J Appl Ichthyol* **22**, 241–253. (doi:10.1111/j.1439-
568 0426.2006.00805.x)
- 569 65. Hernandez-Leon S. 2005 A global assessment of mesozooplankton respiration in the ocean.
570 *Journal of Plankton Research* **27**, 153–158. (doi:10.1093/plankt/fbh166)

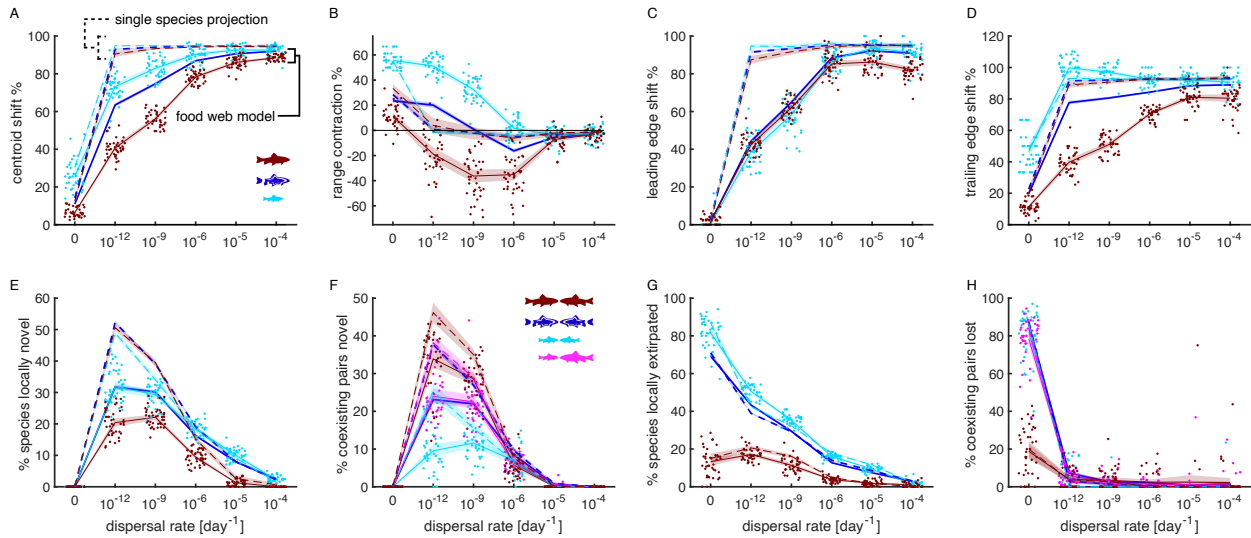
- 571 66. Stuart-Smith RD, Edgar GJ, Bates AE. 2017 Thermal limits to the geographic distributions
572 of shallow-water marine species. *Nature Ecology & Evolution* **1**, 1846–1852.
573 (doi:10.1038/s41559-017-0353-x)

574

575 **Figures**
576



577 **Figure 1. Spatial food-web model.** **A.** The heterotrophic consumer i feeds on other heterotrophs
578 of smaller sizes and, for some consumers, on the basal resource (0.01 g). The rate of biomass
579 flow from one species (j) to another (i) is determined by search rate (v_{ijx}) and handling time (τ_{ix}),
580 which are functions of local temperature T_x , species-specific optimal search temperature $T_{i,opt}$
581 (see example curve), and predator and prey body sizes (s_i, s_j). Metabolic cost (D_{ix}) is dependent
582 on temperature and body size. The food-web is spatially coupled across 21 patches with an initial
583 temperature gradient of 4 to 24 °C. **B.** A snapshot of individual species biomass distributions
584 across patches before warming (dispersal rate $\kappa = 4.5 \times 10^{-9} \text{ day}^{-1}$). **C.** Time series of species
585 biomass at patch 11, which is at 14 °C until year 800 (vertical black line) and warms to 17 °C by
586 year 1000. **D.** A snapshot of individual species biomass distributions across patches after
587 warming. **E-H.** Food webs in four patches (patches 8 to 11) from colder to warmer temperatures
588 along the gradient. Within-patch species are plotted by optimal search temperature (x) and body
589 size (y) traits, with circle area representing biomass (see legend in **H**) and lines representing
590 consumptions above $10^{-5} \text{ gm}^{-3}\text{day}^{-1}$ (line width scaled to log of consumption). Species before
591 warming are shown in blue, and species after warming are shown in red. The blue species in **H**
592 are expected to shift and become the red species in **E** if they keep up with the thermal shift.
593 Overlapping blue and red species with identical centers within patch are those that remain in the
594 original patch after warming. One species (sp.1) is labelled for reference across patches and
595 temperature change.
596



597
 598 **Figure 2. Range shifts and assemblage changes.** Solid lines indicate averages across 40
 599 replicates from the food-web model after warming, while dashed lines indicate corresponding
 600 counterfactual single-species projections. Shades are 95% confidence bounds assuming normal
 601 error. Dots show individual simulations and are jittered on the x-axis to improve readability. Red
 602 indicates species of size 10^5 to 10^6 g, cyan indicates species of size 10^2 to 10^3 g, and blue
 603 indicates all sizes. For coexisting pairs, magenta indicates pairs that contain one small (10^2 to 10^3
 604 g) and one large (10^5 to 10^6 g) species. **A.** Centroid shift measured as the percentage of the
 605 distance that isotherms shifted. **B.** Range contraction. **C.** Leading-edge range-shift measured
 606 relative to isotherm shifts. **D.** Trailing-edge range-shift measured relative to isotherm shifts. **E.**
 607 Percentage of species locally novel, with 100% corresponding to all species after warming being
 608 absent in each patch initially. **F.** Percentage of coexisting pairs novel, with 100% corresponding
 609 to all species pairs after warming being unpaired initially. **G.** Percentage of species locally
 610 extirpated, with 100% corresponding to all species initially in each patch being absent after
 611 warming. **H.** Percentage of coexisting pairs lost, with 100% corresponding to all initial species
 612 pairs being absent after warming.
 613

614 **Tables**

615 **Table 1. Food-web model equations.** Bold symbols are parameters that we vary in this study.
 616 See Table 2 for additional definitions. References for each equation are shown in the first
 617 column. Indices i, j , and k refer to species identity, and x refers to patch location. The
 618 Supplementary Appendix A provides further explanations to the model specifications and
 619 choices.

Definition	Equation	Units
(T1) change in basal resource [61]	$\frac{\Delta B_{0x}}{\Delta t} = F(B_{0max} - B_{0x}) - \sum_{j=1}^N B_{jx} f_{j0x}(B_{0x})$	$\text{gm}^{-3} \text{day}^{-1}$
(T2) functional response [38]	$f_{ijx}(B_{jx}) = \frac{v_{ijx} B_{jx}^2}{1 + \tau_{ix} \sum_{k \neq i} v_{ikx} B_{kx}^2}$	day^{-1}
(T3) dispersal rate to adjacent patches	$\kappa = \frac{m}{A}$	day^{-1}
(T4) active metabolic cost [32,36]	$D_{ix} = C_{W \rightarrow d^{-1}, i} \exp\left(\alpha_D + \beta_D \ln(s_i) - \frac{E_a}{k(T_x + 273)} + c_{\gamma i}\right)$	day^{-1}
(T5) conversion from watts to day ⁻¹	$C_{W \rightarrow d^{-1}, i} = \frac{C_{d \rightarrow s}}{E_c s_i}$	$\text{sj}^{-1} \text{day}^{-1}$
(T6) search rate of species i for species j [12]	$v_{ijx} = \phi_{ij} v_{i, \max} \omega_{ix} / B_r$	$\text{m}^6 \text{day}^{-1} \text{g}^{-2}$
(T7) handling time (species i) [62]	$\tau_{ix} = \frac{\lambda}{\bar{P}_{ix, \max} + D_{ix}}$	day
(T8) metabolic cost factor from swimming [36]	$c_{\gamma i} = R_{es} \gamma_i$	
(T9) maximum search rate at reference prey density [36]	$v_{i, \max} = \frac{F_h \pi l_i^2 \gamma_i}{s_i}$	$\text{m}^3 \text{day}^{-1} \text{g}^{-1}$
(T10) feeding kernel [63]	$\phi_{ij} = \frac{\exp\left(\frac{-(\log_{10} s_i - \log_{10} s_j - M_i)^2}{2\sigma^2}\right)}{\sqrt{2\pi}\sigma}$	
(T11) maximum production rate [62]	$\bar{P}_{ix, \max} = \frac{1000 \cdot 10^{\alpha_p}}{365 s_i} \left(\frac{s_i}{1000}\right)^{\beta_p} \exp\left(\frac{-E_a}{k(T_x + 273)}\right)$	day^{-1}
(T12) swim speed [36]	$\gamma_i = \frac{1.0 \cdot C_{d \rightarrow s} s_i^{\beta_\gamma}}{100}$	m day^{-1}
(T13) body length [64]	$l_i = \frac{\left(\frac{s_i}{\alpha_l}\right)^{\frac{1}{\beta_l}}}{100}$	m
(T14) log ₁₀ mean predator-prey mass ratio [31]	$M_i = \alpha_R + \beta_R \log_{10} s_i$	
(T15) Skew normal function [12]	$\omega_{ix} = \theta \exp\left(-\frac{(T_x - T_{i, \text{opt}} - T_{\text{oset}})^2}{2w_T^2}\right) \left(1 + \text{erf}\left(\xi \frac{T_x - T_{i, \text{opt}} - T_{\text{oset}}}{\sqrt{2}w_T}\right)\right)$	

620
621

622 **Table 2. Parameter definitions.** Bold symbols are parameters that we vary in our analyses.
 623 Values in parentheses are the alternative parameter values, with † to indicate the value used in
 624 Figure S4 (other alternative values are shown in Figures S5-S7). See Supplementary Appendix
 625 A.

Symbol	Definition	Value
A	patch area [m^2]	471,429 ²
α_D	body size to metabolic rate power-law constant	18.47 [32]
α_l	body length-mass power-law constant	0.012 [64]
α_P	body size to biomass production power-law constant	10.85 [62]
α_R	body size to predator-prey mass ratio power-law constant	2.66 (2.08[†], 2.37, 2.95, 3.24) [31]
β_D	body size to metabolic rate scaling exponent	0.71 [32]
β_γ	body size-swim speed scaling exponent	0.13 [36]
β_l	body length-mass scaling exponent	3 [64]
β_P	body size to biomass production scaling exponent	0.761 [62]
β_R	body size-predator-prey mass ratio scaling exponent	0.24 [31]
B_{0max}	maximum basal biomass [g m^{-3}]	5 [37]
B_r	reference prey biomass [g m^{-3}]	1
$C_{d \rightarrow s}$	conversion factor from days to seconds [s/day]	86400
E_a	activation energy [eV]	0.63 (0.57, 0.6, 0.66, 0.69[†]) [32]
E_c	energetic content of organisms [Jg^{-1}]	7000 [56]
F	basal chemostatic dilution rate [day^{-1}]	0.0075 [65]
F_h	fraction of time hunting	0.26 (0.13[†]) [43]
k	Boltzmann's constant [$\text{eV}^\circ\text{C}^{-1}$]	8.62×10^{-5}
λ	consumption efficiency	0.4 (0.2[†]) [44]
m	diffusion coefficient [$\text{m}^2 \text{day}^{-1}$]	0, 1, 10³, 10⁶, 10⁷, 10⁸
N	number of heterotroph species	200
σ	width of feeding kernel	0.569 [63]
P_N	percent of prey inedible	0 (10, 20[†], 30, 40, 50)
R_{es}	coefficient for swimming cost [day/m]	3.47×10^{-5} [36]
s	body mass [g]	0.01, 10 ¹ -10 ⁶
T_x	local temperature [$^\circ\text{C}$]	4 – 24 (+3)
$T_{i,opt}$	optimal search temperature [$^\circ\text{C}$] for species i	0 – 34
T_{oset}	optimal search temperature offset to align the skew normal mode with $T_{i,opt}$ [$^\circ\text{C}$]	0.435
w_T	search performance standard deviation [$^\circ\text{C}$]	0.884 [66]
θ	search rate scaling factor so that skew normal function is 1 at $T_{i,opt}$	0.622
ξ	thermal performance skew	-2.7 [12]

626